Journal of Alloys and Compounds 513 (2012) 202–207

Contents lists available at SciVerse ScienceDirect

Journal of Alloys and Compounds

journal homepage: www.elsevier.com/locate/jallcom

# Effect of niobium particulate addition on the microstructure and mechanical properties of pure magnesium

M. Shanthi [a,*], P. Jayaramanavar [b], V. Vyas [c], D.V.S. Seenivasan [a], M. Gupta [a]

[a] *Department of Mechanical Engineering, National University of Singapore, 10, Kent Ridge Crescent, Singapore 119260, Singapore*
[b] *Department of Metallurgical & Materials Engineering, Malaviya National Institute of Technology, Jaipur 303017, India*
[c] *Department of Metallurgical & Materials Engineering, National Institute of Technology, Durgapur 713209, India*

ARTICLE INFO

*Article history:*
Received 29 April 2011
Received in revised form 1 October 2011
Accepted 7 October 2011
Available online 17 October 2011

*Keywords:*
Metal matrix composites
Microstructure
Mechanical properties
Scanning electron microscopy
X-ray diffraction

ABSTRACT

Magnesium based composites containing 5–15 wt% niobium particulates were synthesized using disintegrated melt deposition technique. Microstructural characterization revealed reasonably uniform distribution of niobium particulates in the matrix with no intermetallics formation, reasonable grain refinement and minimal porosity. Mechanical characterization under tensile loading revealed simultaneous improvement in hardness, 0.2% yield strength and ultimate tensile strength up to 10 wt% Nb, while ductility was compromised beyond 5 wt% niobium particulate addition to pure magnesium. The optimal composition with good combination of strength and ductility is observed at Mg/5 wt% Nb composite while the best improvement in strength and hardness among the composites was observed only for Mg–10 wt% Nb composite.

© 2011 Elsevier B.V. All rights reserved.

## 1. Introduction

Magnesium and its alloys have been developed in large spectrum in recent years and have attracted significant interest of researchers due to their high strength–weight ratio. This makes them highly essential materials in replacing heavier parts in automobile applications and structural parts in electronic devices [1,2]. However, the limitations of magnesium and its alloys include poor corrosion resistance and limited mechanical properties at high service temperature [3,4]. To overcome these limitations, alloying of magnesium with different elements has been attempted. Results revealed that the addition of various elements such as Bi, Sb, Y and rare earth element to magnesium and its alloys matrix has shown to improve the strength of magnesium even at high temperatures [5–8].

Apart from the alloying technique, addition of reinforcements to magnesium and its alloy matrix to form composites has attracted special attention because of their superior mechanical properties, good corrosion resistance and high temperature creep resistance [9–11]. Addition of micron size ceramic particulates such as SiC and $Al_2O_3$ to the magnesium matrix has resulted in improved strength with compromise in ductility [12–15]. To improve ductility, few attempts have been made to reinforce metallic particulates such as titanium, titanium alloy, and copper to pure magnesium matrix [16–21]. Results revealed that titanium/titanium alloy reinforced magnesium matrix composites has showed improved ductility compared to ceramic particulates reinforced magnesium composites.

In this current study, attempt has been made to add refractory material niobium to the magnesium matrix. It should be noted that no reports from the open literature are available for such composites. The exceptional property of niobium includes low density ($8.57\,g/cm^3$) compared to other refractory metals such as tantalum $16.6\,g/cm^3$ and molybdenum $10.2\,g/cm^3$ (high melting point metals). Moreover, niobium is completely immiscible with magnesium which indicates that the formation of brittle intermetallic phases at the magnesium–niobium interface can be avoided. Apart from this, niobium also exhibits good corrosion resistant, good thermal stability and easy availability with low cost compared to other commonly used refractory metal tantalum. Niobium is also extensively used in aerospace equipment and missiles because of its relatively light weight and high temperature stability. Furthermore niobium is resistant to most organic and mineral acid below $100\,^{\circ}C$ and inert to most common gases up to $100\,^{\circ}C$ [22]. These unique properties make niobium a suitable reinforcement for magnesium.

Accordingly, the aim of the present study is to synthesize the niobium particulate reinforced magnesium composite using disintegrated melt deposition technique. The effect of niobium

---

* Corresponding author. Tel.: +65 6516 6358; fax: +65 6779 1459.
*E-mail address:* shanthimuthusamy@gmail.com (M. Shanthi).

0925-8388/$ – see front matter © 2011 Elsevier B.V. All rights reserved.
doi:10.1016/j.jallcom.2011.10.019

particulate addition on the microstructure and mechanical properties of the composites were investigated.

## 2. Experimental procedures

### 2.1. Primary processing

#### 2.1.1. Materials

In the present study, pure magnesium turnings of >99.9% purity (supplied by ACROS Organics, New Jersey, USA) were used as base material and niobium powder of 99% purity (supplied by Rockford, IL, USA) with an average size of <10 μm was used as reinforcement phase.

#### 2.1.2. Disintegrated melt deposition technique

Synthesis of Mg–Nb composite was carried out using the disintegrated melt deposition technique. The processing step involves the melting and superheating of magnesium turnings with niobium particulates to 750 °C under inert argon gas atmosphere in a graphite crucible using the resistance heating furnace. Upon reaching the superheat temperature, the molten slurry was stirred at 460 rpm using a zirtex coated twin blade (pitch 45°) stirrer to facilitate the incorporation and uniform distribution of reinforcement particulates in the metallic melt. The melt was then released through a 10 mm diameter orifice at the base of the crucible which was equipped with bottom pouring facility and was disintegrated by two jets of argon gas orientated normal to the melt stream. The disintegrated composite melt slurry was subsequently deposited onto a metallic substrate forming ingots of 40 mm diameter. The synthesis of monolithic magnesium without the addition of reinforcements was carried out using the same procedure for comparison purposes.

### 2.2. Secondary processing

The cast ingots obtained at the deposition stage were machined to 36 mm diameter and hot extruded at 350 °C using an extrusion ratio of 20.25:1 on a 150 ton hydraulic press. These cast ingots were held in a resistance heating furnace at a constant temperature of 400 °C for 60 min before extrusion. Colloidal graphite was used as a lubricant and to prevent oxidation. Rods of 8 mm diameter were obtained after extrusion.

### 2.3. Density measurement

The density of pure magnesium and its composites was measured using the Archimedes' Principle on three randomly selected polished samples. Distilled water was used as the immersion fluid. The weight of the samples in air and water was measured using an electronic balance (AND HM-202), with an accuracy of ±0.0001 g. Theoretical densities of the samples were calculated using rule-of-mixture.

### 2.4. Microstructure characterization

Microstructural characterization studies were conducted on metallographically polished extruded samples to determine grain size, grain morphology, distribution of reinforcement within the matrix and porosity. An OLYMPUS optical microscope and Hitachi S4300 Field-Emission Scanning Electron Microscope (FESEM) equipped with EDS was used. Scion Image Analyser system was used to determine the grain size of magnesium and its composites.

### 2.5. X-ray diffraction

X-ray diffraction studies were carried out on the polished samples of pure Mg and Mg/Nb composites using automated Shimadzu XRD-6000 diffractometer to identify the phases present in the materials. The samples were exposed to CuK$_\alpha$ radiation ($\lambda = 0.15418$ nm) at a scanning speed of 2°/min to measure the Bragg angles ($\theta$) and inter-planar spacing ($d$).

### 2.6. Hardness

Microhardness measurements were performed on the polished Mg and Mg/Nb samples using a Matsuzawa MXT50 automatic digital microhardness tester. The test was performed using the Vickers indenter under a load of 25 gf with 15 s dwell time in accordance with ASTM E384-99 standard.

### 2.7. Tensile testing

The tensile properties of the extruded pure Mg and Mg/Nb composites were determined in accordance with ASTM test method E8M-08 using MTS 810 tensile testing machine. The test was conducted on a round tension test specimens of 5 mm diameter and 25 mm gauge length with a cross-head speed set at 0.254 mm/min. A total of five tensile samples were tested for each material. MTS extensometer was used for strain recording.

**Table 1**
Results of density and porosity measurements of pure Mg and Mg/Nb composites.

| Composition | Nb (wt%) | Density (g/cm$^3$) | | Porosity (%) |
|---|---|---|---|---|
| | | Theoretical | Experimental | |
| Pure Mg | 0 | 1.740 | 1.7383 ± 0.0018 | 0.10 |
| Mg–5 wt% Nb | 5 | 1.812 | 1.7957 ± 0.0023 | 0.90 |
| Mg–10 wt% Nb | 10 | 1.890 | 1.8772 ± 0.0022 | 0.69 |
| Mg–15 wt% Nb | 15 | 1.975 | 1.9645 ± 0.0058 | 0.56 |

### 2.8. Fractography

Fracture surface of the tensile samples was analyzed using a JEOL JSM-5600LV scanning electron microscope (SEM) and Hitachi S4300 Field-Emission Scanning Electron Microscope (FESEM) to investigate the fracture mechanisms operative under tensile loading for both pure magnesium and its composites.

## 3. Results

### 3.1. Macrostructural characteristics

Macrostructural characterization conducted on the as-deposited and extruded rods of pure Mg and Mg/Nb composites did not reveal any blowholes, shrinkage cavity and macropores. This shows the capability of the processing technique to produce cast ingots with no processing defects.

### 3.2. Density measurements

The results of the density and porosity measurements are listed in Table 1. Results reveal that near dense pure Mg and Mg/Nb samples can be obtained using the current fabrication technique. This was further supported by the presence of minimal porosity below 1% in the samples.

### 3.3. Microstructural characteristics

Microstructural characterization conducted on Mg/Nb composites revealed fairly uniform distribution of niobium particulates in pure magnesium matrix for Mg–5 wt% Nb and Mg–10 wt% Nb composites (Fig. 2a and b). However, for Mg–15 wt% Nb composites, severe clustering of niobium particulates was observed as shown in Fig. 2c. The results of grain size and grain morphology of pure Mg and Mg/Nb samples are shown in Table 2. For both monolithic magnesium and its composites, near-equiaxed grain morphology was observed.

### 3.4. X-ray diffraction

Results of the X-ray diffraction analysis obtained from pure Mg and Mg/Nb composites are shown in Fig. 3. Diffractograms indicated the presence of magnesium peaks for pure magnesium sample and magnesium and niobium peaks for Mg/Nb composites. No intermetallic formation was observed.

**Table 2**
Results of grain size and grain morphology of pure Mg and Mg/Nb composites.

| Materials | Grain size (μm) | Aspect ratio | Roundness (μm) |
|---|---|---|---|
| Pure Mg | 16.3 ± 8 | 1.84 ± 0.68 | 1.93 ± 0.94 |
| Mg–5 wt% Nb | 9.1 ± 3.2 | 1.82 ± 0.63 | 1.91 ± 0.65 |
| Mg–10 wt% Nb | 13.4 ± 6.3 | 1.97 ± 0.98 | 1.95 ± 0.93 |
| Mg–15 wt% Nb | 9.7 ± 5 | 2.14 ± 1.01 | 1.98 ± 0.90 |

**Table 3**
Results of room temperature tensile properties of pure Mg and Mg/Nb composites.

| Materials | Microhardness (HV) | 0.2% YS (MPa) | UTS (MPa) | Failure strain (%) | Work of fracture (MJ/$m^3$) |
|---|---|---|---|---|---|
| Pure Mg | 46 ± 2 | 128 ± 3 | 174 ± 5 | 8.1 ± 0.4 | 13.8 ± 1 |
| Mg–5 wt% Nb | 45 ± 2 | 129 ± 5 | 186 ± 5 | 13.4 ± 1.1 | 24.3 ± 2.3 |
| Mg–10 wt% Nb | 51 ± 2 | 186 ± 5 | 238 ± 4 | 4.3 ± 0.8 | 10.5 ± 2.1 |
| Mg–15 wt% Nb | 46 ± 2 | 162 ± 13 | 193 ± 21 | 2.2 ± 0.7 | 5.4 ± 1.5 |

### 3.5. Microhardness

The results of microhardness measurements conducted on the polished samples of pure Mg and Mg/Nb composites are presented in Table 3. Results revealed that an increase in average microhardness (see Table 3) with increase in niobium particulate was realised only in Mg–10 wt% Nb composite. Beyond 10 wt% Nb addition, no considerable change in microhardness was observed compared to pure magnesium.

### 3.6. Tensile characteristics

Results of the mechanical properties obtained under tensile testing condition are presented in Table 3. Tensile test conducted on Mg–Nb composites revealed an improvement in 0.2% yield strength and ultimate tensile strength up to10 wt% niobium particulate addition to magnesium matrix. However, drop in 0.2% yield strength and ultimate tensile strength was observed in Mg–15 wt% Nb composites compared to Mg–10 wt% Nb composites. It should be noted that the yield strength and ultimate tensile strength of Mg/15 wt% Nb composites still remained higher than monolithic magnesium and Mg/5 wt% Nb composites. In general, the addition of niobium particulate to the magnesium matrix has resulted in improved strength in case of Mg/Nb composites. The improvement in ductility compared to pure magnesium was observed only at 5 wt% Nb particulate addition, beyond which the ductility is adversely affected. Work of fracture for composites is higher only for Mg/5 wt% Nb composites compared to pure magnesium and other composites.

### 3.7. Fracture behaviour

Fracture surfaces of monolithic magnesium and Mg/Nb composites are shown in Fig. 4. Tensile fracture surface of pure magnesium showed mixed ductile and brittle fracture (see Fig. 4a). In case of Mg/5 wt% Nb composites, more evidence of plastic deformation with fine dimple like features was observed (see Fig. 4b). With increase in niobium particulates addition beyond 5 wt%, the fracture surface changed from ductile fracture to microscopically rough surface with limited evidence of plastic deformation. The presence of micro cracks was observed in Mg–10 wt% Nb and Mg–15 wt% Nb composites (Fig. 4c and d).

## 4. Discussion

### 4.1. Microstructural characterization

Microstructural characterization of the extruded samples revealed nearly equiaxed grains as shown in Fig. 1. Results obtained from grain size measurement revealed that the addition of niobium particulates to the magnesium matrix has resulted in reasonable grain refinement (see Table 2). This suggests that the presence of niobium particulates can act as an obstacle or nucleation site to the grain growth during solid state cooling resulting in grain refinement. The presence of minimal porosity can be related to the good compatibility between the matrix and reinforcement and proper selection of extrusion parameters.

Results of FESEM micrograph reveal uniform distribution of niobium particulates in the magnesium matrix as shown in Fig. 2a and b. The uniform distribution of the reinforcement can be related to the uniform arrangement of reinforcement and matrix materials, good wettability between the matrix and reinforcement and proper stirring parameter during casting. However, clustering of niobium particulates slightly initiates at Mg–10 wt% Nb composites and becomes more evident in Mg–15 wt% Nb composite as shown in Fig. 2c. This suggests that addition of niobium particulates beyond 10 wt% can result in severe agglomeration of reinforcement particles in the matrix. No intermetallic formation is observed in Fig. 2a–c. This was supported by the XRD results indicating the absence of any reaction between the magnesium matrix and reinforcement as shown in Fig. 3. This is due to the limited solid solubility of niobium in magnesium as supported by Mg–Nb phase diagram [23]. Absence of intermetallic formation was reported in earlier studies of Ti metallic particulate reinforced magnesium composites [16,19]. Interfacial integrity between the matrix and reinforcement was observed to be good and no interfacial debonding was observed as shown in Fig. 2d.

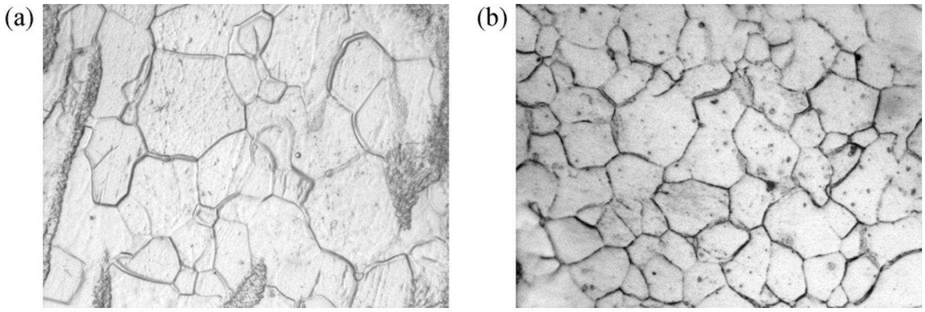

**Fig. 1.** Representative micrographs showing equiaxed grain morphology at 500× magnification for: (a) monolithic magnesium and (b) Mg–5 wt% Nb composite.

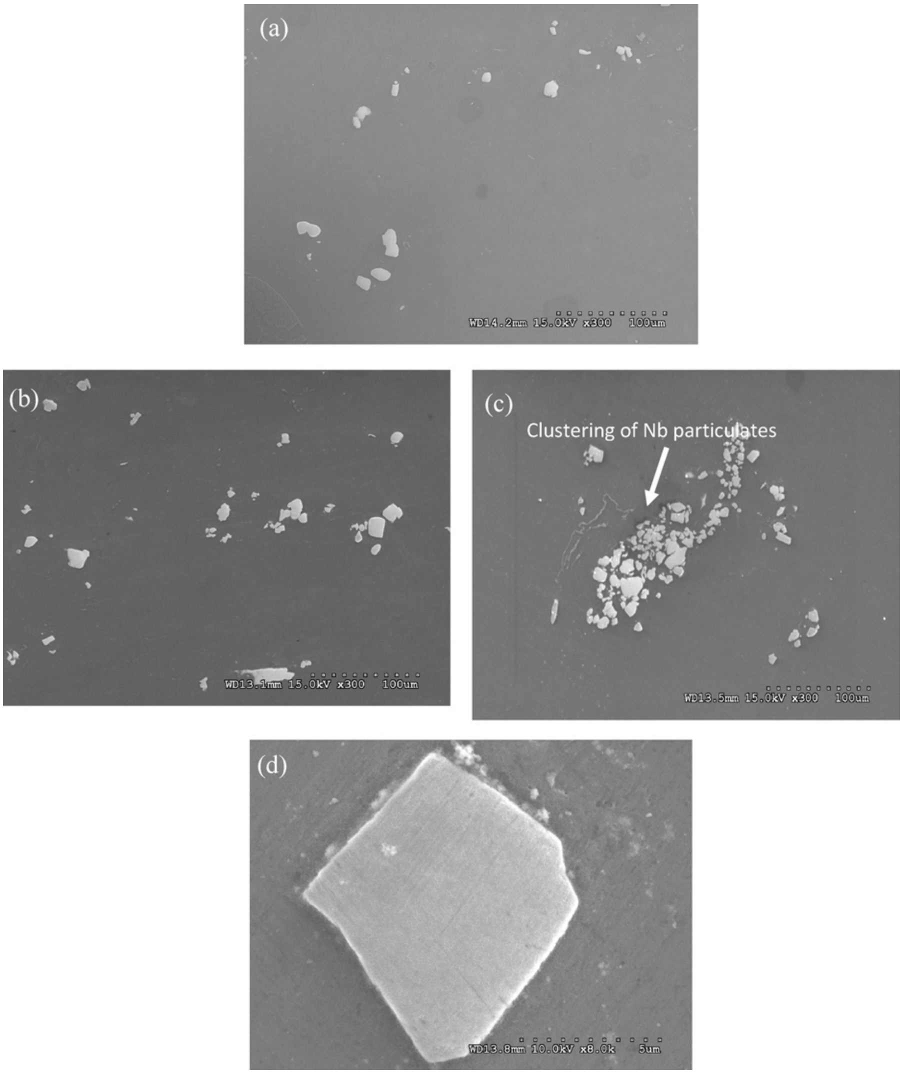

**Fig. 2.** Representative FESEM micrographs showing reasonably uniform distribution of niobium particulate reinforcement in: (a) Mg/5 wt% Nb, (b) Mg/10 wt% Nb composites, (c) severe clustering of reinforcement particulates in Mg/15 wt% Nb composites and (d) interfacial integrity between the niobium particulate and magnesium matrix.

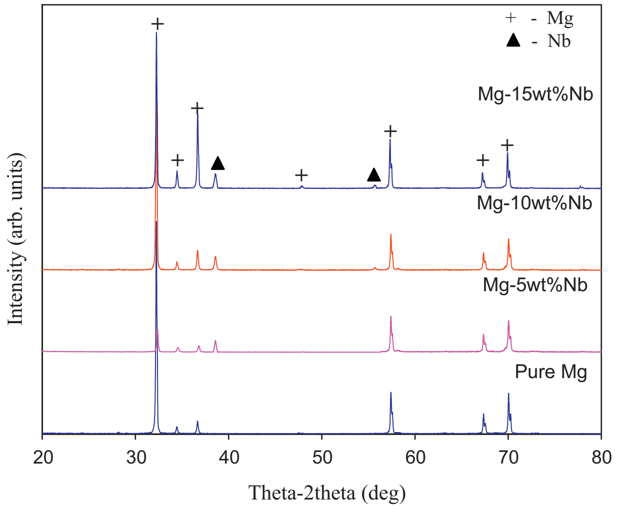

**Fig. 3.** XRD peaks showing the presence of Mg in monolithic magnesium and Mg and Nb in Mg–(5–15) wt% Nb composites.

### 4.2. *Mechanical behaviour*

Results of the microhardness measurement revealed that addition of 5 wt% Nb particulates to magnesium matrix was not sufficient enough to increase the hardness of the composite while improvement in hardness of 11% was realised only at Mg/10 wt% Nb composite compared to monolithic magnesium. The improvement in hardness observed at 10 wt% addition can be primarily attributed to (a) reasonably uniform distribution of the niobium particulates, (b) grain refinement [24] and (c) high constraint to localized matrix deformation due to the presence of refractory niobium particulates [25]. Similar improvement in macrohardness by the addition of ductile copper particulates to magnesium matrix was reported earlier [18]. In case of Mg/15 wt% Nb composite, no significant change in hardness was observed compared to monolithic magnesium. This could be due to the severe clustering of niobium particulates at the grain boundaries when added beyond 10 wt% niobium particulates to magnesium matrix. Out of three compositions studied, Mg/10 wt% Nb composite showed better improvement in hardness compared to other composites.

The results of room temperature tensile testing showed improvement in 0.2% yield strength and ultimate tensile strength of pure magnesium with increase in niobium particulate addition up to 10 wt%. The improvement in strength can be attributed to (a)

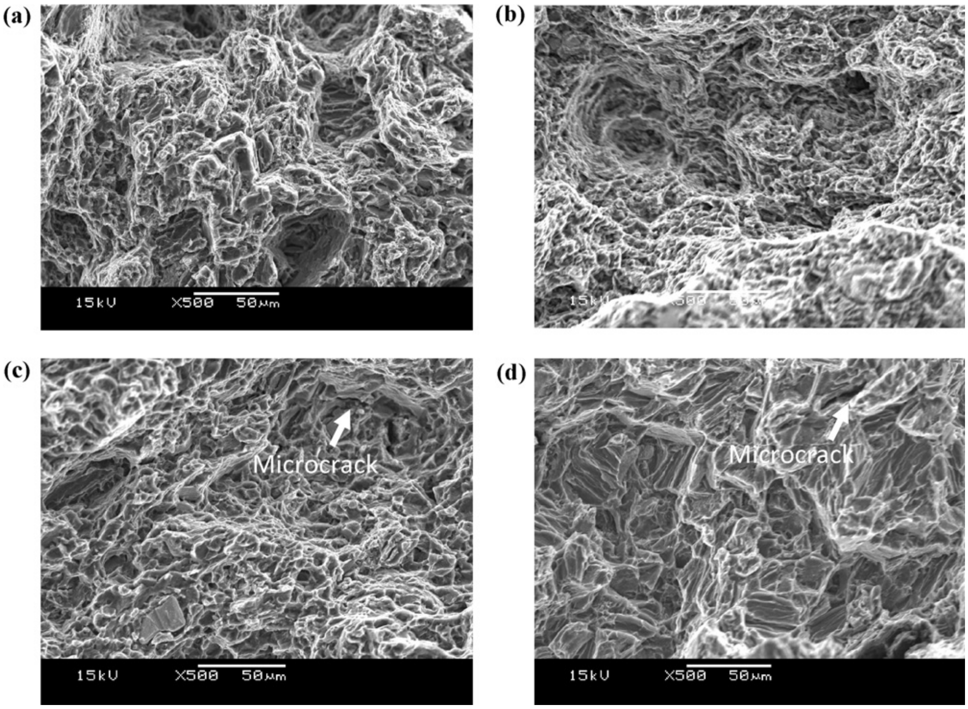

**Fig. 4.** Representative FESEM fractographs: (a) mixed ductile and brittle fracture in pure Mg, (b) more plastic deformation and fine dimple like features in Mg/5 wt% Nb composite, (c) less evidence of plastic deformation with micro cracks evident in Mg/10 wt% Nb composite and (d) rough surface with more cleavage planes and micro cracks Mg/15 wt% Nb composite.

an increase in dislocation density in the matrix due to their large CTE differences with respect to magnesium ($24.8 \times 10^{-6}/^{\circ}C$ and $7.3 \times 10^{-6}/^{\circ}C$ for Mg and Nb [26]), (b) effective transfer of applied tensile load due to the presence of well bonded reinforcements in the matrix ($E = 44.7$ and $E = 103$ GPa for Mg and Nb [27]) and (c) grain refinement [24]. Thus under applied stress, niobium second phase particulates and increasing amount of grain boundaries in the matrix act as a barrier to dislocation movement resulting in dislocation pile up. Thus the coupled effect of these obstacles has resulted in high yield strength of the composites. In general, improvement in strength compared to pure magnesium was noticed in all three composites. However, the best 0.2% yield strength and ultimate tensile strength with 45% and 37% improvement was observed in Mg–10 wt% Nb composite. This improvement clearly supports that initiation of mild clustering (see Fig. 2b) noted in Mg–10 wt% Nb composites has no effect on the strength of the composites under tensile loading condition.

Tensile property characterization revealed that the ductility of the composites showed improvement over pure magnesium only at Mg–5 wt% Nb composite, beyond which the ductility is adversely affected. Similar observation of increase in ductility was reported in titanium particulate reinforced magnesium composites [19]. The improvement in ductility can be related to the following factors: (a) the ductile niobium reinforcement present in matrix which deforms upon yielding and uniformly transfers the applied load across the sample which delays early crack nucleation and propagation and (b) reducing the stress build up at the matrix–particle interface leading to overall matrix–particle interfacial relaxation resulting in improved ductility. This observation was supported by earlier studies [28,29]. The adverse effect of ductility beyond Mg–5 wt% Nb composite can be related to clustering of niobium particulates in the matrix which might serve as crack nucleation sites leading to reduction in ductility under tensile loading conditions. Similar observation of reduced failure strain was reported in ZK60/1.5$Al_2O_3$ nanocomposites due to the agglomeration of nano particulates in the matrix [29]. Work of fracture corresponds to ability of the material to absorb energy up to fracture under load [30]. Work of fracture improved to about 76% in Mg–5 wt% Nb composite compared to pure magnesium. This corresponds to the higher ductility exhibited by Mg–5 wt% Nb composite.

### 4.3. *Fracture behaviour*

Fracture surface analysis conducted on the tensile surface of magnesium revealed mixed ductile and brittle like feature which is consistent with the relatively higher ductility exhibited by pure magnesium compared to Mg–10 wt% and Mg/15 wt% Nb composite (see Table 3 and Fig. 4a). However for Mg–5 wt% Nb composite, fracture surface revealed predominately ductile type fracture with fine dimple like features and more evidence of plastic deformation. These features are consistent with the high ductility exhibited by the Mg–5 wt% Nb composite. With increase in niobium particulate addition, the ductility is adversely affected. The presence of micro cracks was observed in both Mg–(10–15) wt% Nb composites (see Fig. 4c and d). Fracture surface of Mg–(10–15) wt% Nb composite showed limited evidence of plastic deformation with microscopically rougher surface and cleavage like features (especially in Mg–15 wt% Nb) compared to pure magnesium which is consistent with the poor ductility exhibited by these composites.

In summary, for Mg–Nb composites, the optimal composition showing good combination of reasonable strength (improved UTS and a slight improvement in 0.2% YS) and enhanced ductility is observed at Mg–5 wt% Nb composite. However, excellent improvement in 0.2% yield strength and ultimate tensile strength is observed only at Mg–10 wt% Nb composite. Hence Mg–5 wt% Nb composite can be used for applications requiring moderate strength and enhanced ductility whereas Mg–10 wt% Nb composite can be used in strength based applications with compromise in ductility.

### 4.4. Conclusions

1. Niobium particulates reinforced magnesium composites can be successfully synthesized using the disintegrated melt deposition technique coupled with hot extrusion.
2. Microstructural characterization of Mg/Nb composites revealed reasonably uniform reinforcement distribution of niobium particulates with good interfacial integrity, reasonable grain refinement and minimal porosity.
3. Mechanical property characterization under tensile loading conditions revealed improvement in hardness, 0.2% yield strength and ultimate tensile strength, up to Mg–10 wt% Nb composite. Enhancement in ductility was observed only at Mg–5 wt% Nb composite beyond which ductility is adversely affected compared to pure magnesium.
4. Fractography studies revealed that fracture surface of pure magnesium showed mixed ductile and brittle fracture mode which eventually changed to predominately ductile type fracture with fine dimple like features for Mg–5 wt% Nb composites. For Mg–(10–15) wt% Nb composite, the fracture surface revealed micro cracks and microscopically rough surface with less evidence of plastic deformation.
5. The optimal composition showing reasonable strength and better ductility is observed to be Mg–5 wt% Nb composite whereas the best improvement in hardness and strength is observed at Mg–10 wt% Nb composite.

## Acknowledgement

Authors wish to acknowledge National University of Singapore for funding this research through grants and studentships.

## References

[1] B.L. Mordike, T. Ebert, Mater. Sci. Eng. A 302 (2001) 37–45.
[2] Y. Kojima, S. Kamado, Mater. Sci. Forum 488–489 (2005) 9–16.
[3] G.Y. Yuan, Y.S. Sun, W.J. Ding, Mater. Sci. Eng. A 308 (2001) 38–44.
[4] G. Wu, Y. Fan, H. Gao, C. Zhai, Y.P. Zhu, Mater. Sci. Eng. A 408 (2005) 255–263.
[5] S.Y. Chang, T. Nakagaido, S.K. Hong, D.H. Shin, T. Sato, Mater. Trans. JIM 42 (2001) 1332–1338.
[6] T. Mohri, M. Mabuchi, N. Saito, M. Nakamura, Mater. Sci. Eng. A 257 (1998) 287–294.
[7] X. Wang, X. Zeng, G. Wu, S. Yao, Y. Lai, Appl. Surf. Sci. 253 (2007) 3574–3580.
[8] Y.Q. Wang, K. Wu, M.Y. Zheng, Surf. Coat. Technol. 201 (2006) 353–360.
[9] M. Mabuchi, K. Kubota, K. Higashi, Scr. Metall. Mater. 33 (1995) 331–334.
[10] M. Russell-Stevens, D.C. Plane, J. Summerscales, P. Schulz, M. Papakyriacou, Mater. Sci. Technol. 18 (2002) 501–506.
[11] A. Feng, Y. Han, J. Alloys Compd. 504 (2010) 585–593.
[12] M. Gupta, L. Lu, M.O. Lai, K.H. Lee, MRS Bull. 34 (1999) 1201–1214.
[13] M. Gupta, M.O. Lai, D. Saravanaranganathan, J. Mater. Sci. 35 (2000) 2155–2165.
[14] S.F. Hassan, M. Gupta, J. Alloys Compd. 419 (2006) 84–90.
[15] G. Huard, R. Angers, M.R. Krishnadev, R. Tremblay, D. Dube, Can. Metall. Q. 38 (1999) 193.
[16] P. Perez, G. Garces, P. Adeva, Compos. Sci. Technol. 64 (2004) 145–151.
[17] L. Lu, M.O. Lai, Y.H. Toh, L. Froyen, Mater. Sci. Eng. A 334 (2002) 163–172.
[18] S.F. Hassan, M. Gupta, Mater. Res. Bull. 37 (2002) 377–389.
[19] S.F. Hassan, M. Gupta, J. Alloys Compd. 345 (2002) 246–251.
[20] Y.L. Xi, D.L. Chai, W.X. Zhang, J.E. Zhou, Scr. Mater. 54 (2006) 19–23.
[21] J. Umeda, M. Kawakami, K. Kondoh, EL-S. Ayman, H. Imai, Mater. Chem. Phys. 123 (2010) 649–657.
[22] ASM Speciality Handbook, Magnesium and Magnesium Alloys, ASM International, 1999, p. 37.
[23] J.F. Smith, in: T.B. Massalski (Ed.), Mg–Nb (Magnesium–Niobium), Binary Alloy Phase Diagrams, vol. 3, 2nd ed., 1990, p. 2526.
[24] B. Jing, S. Yangshan, X. Feng, X. Shan, Q. Jing, T. Weijian, Scr. Mater. 55 (2006) 1163–1166.
[25] P.O. Kettunen, V.-T. Kuokkala, Plastic Deformation and Strain Hardening, Trans Tech, Enfield, NH, 2002.
[26] C.J. Smithells, Metals Reference Book, 7th ed., Butterworth-Heinemann, London, 1992, pp. 14-1, 14-2, 14-22, 14-5.
[27] ASM Handbook: Properties and Selection: Non-ferrous Alloys and Special-purpose Materials, vol. 2, ASM International, Materials Park, OH, 1990, p. 1144.
[28] S.C.V. Lim, M. Gupta, Mater. Sci. Technol. 19 (2003) 803–808.
[29] P. Jayaramanavar, M. Paramsothy, A. Balaji, M. Gupta, J. Mater. Sci. 45 (2010) 1170–1178.
[30] R.E. Reed-Hill, Physical Metallurgy Principles, 2nd ed., D Van Nostrand Company, New York, 1964, pp. 192, 267, 725.